Available online at www.sciencedirect.com
SCIENCE DIRECT
Catalysis Today 107–108 (2005) 77–85
CATALYSIS TODAY
www.elsevier.com/locate/cattod

Effect of mileage on the deactivation of vehicle-aged three-way catalysts

M. López Granados [a,*], C. Larese [a], F. Cabello Galisteo [a], R. Mariscal [a], J.L.G. Fierro [a], R. Fernández-Ruíz [b], R. Sanguino [c], M. Luna [c]

[a] *Instituto de Catálisis y Petroleoquímica (CSIC), C/Marie Curie, 2, Campus de Cantoblanco, 28049 Madrid, Spain*
[b] *Servicio Interdepartamental de Investigación, Universidad Autónoma de Madrid, Cantoblanco, 28049 Madrid, Spain*
[c] *Departamento de Homologación de Ford España, C/Caléndula, 13, Edif. MINIP IV, La Moraleja, 28109 Madrid, Spain*

Available online 16 August 2005

Abstract

Two used three-way catalysts (TWC) removed from the same type of automobiles but with different mileages were characterised (by XRD, TPR, N_2 adsorption and TXRF) and their catalytic properties were tested. Both used catalysts were clearly deactivated, especially as regards the elimination of NO and propylene. CO oxidation was much less affected. The data on activity suggest that the rate of deactivation slows down beyond a certain mileage. Attention was focused on the changes brought about by mileage in the textural properties, the deposition of contaminants (mainly P, Zn and Pb), the alteration of the reducibility of Ce oxide and the formation of phases between contaminants and washcoat components ($CePO_4$ and $Zn_2P_2O_7$). The results were compared with those from a fresh counterpart catalyst. The dependence of all the above effects on mileage and the impact on the deactivation of catalytic activity is discussed critically. It is suggested that although other effects may play a secondary role in the used TWC catalysts studied in this work Pb poisoning exerts a definitive impact on the deactivation of the catalytic activity.
© 2005 Elsevier B.V. All rights reserved.

Keywords: Vehicle-aged TWCs; Deactivation; OSC damage; Pb poisoning; Thermal aging; $CePO_4$

1. Introduction

Car manufacturers have been forced to take measures in order to reduce the toxic gases emitted by vehicle exhaust pipes. Gasoline-driven cars can only comply with permitted levels by installation of the so-called ''three-way catalysts'' (TWC) [1–3]. These catalysts undergo diverse deactivation processes that lead to a loss of efficiency and limit their duration. Any improvement in TWC stability must be based on knowledge of the causes of deactivation that operate under real driving conditions. Extensive research has concentrated on the temperature-driven causes of deactivation (sintering of active sites) [4–7], while less attention has been devoted to other causes related to the deposition of certain compounds on the catalyst that are carried by the exhaust gases [8,9]. The aim of the present work is to contribute to unveiling the causes of deactivation in TWCs by studying catalysts that have been subjected to aging under real conditions. The authors have identified several effects brought about by the functioning of TWCs under real traffic conditions: deposition of P, Zn, Ca and Pb, loss of surface area, $CePO_4$ formation and loss of noble metals by erosion [10–12]. Although several mechanisms can be invoked to explain how the above effects can deactivate the catalyst, their impact on deactivation remains to be fully elucidated. Owing to the complexity of the composition of TWCs and the complex network of chemical reactions that result in the elimination of toxic gases and that may be affected by the hypothetical causes of deactivation, the answer to this issue is not straightforward.

Here, we address two traffic-aged catalysts from the same type of car model but with different mileage. They were supplied by the Department of Homologation of Ford, Spain.

* Corresponding author.
E-mail address: mlgranados@icp.csic.es (M. López Granados).

0920-5861/$ – see front matter © 2005 Elsevier B.V. All rights reserved.
doi:10.1016/j.cattod.2005.07.064

This choice was based on our aim to achieve better control of the driving conditions (a mainly urban driving mode, the same type of lubricant and gasoline, the same type of engine, etc.) and operation variables that the catalysts had been subjected to. The aged catalysts were characterised by techniques that have demonstrated their appropriateness in this type of studies [10–12], i.e. X-ray diffraction (XRD), total reflection X-ray fluorescence (TXRF), temperature programmed reduction (TPR) and N_2 adsorption isotherms. A fresh catalyst with 0 km was also studied as a reference. The study was accomplished in the belief that the result should contribute to knowledge of the true causes of deactivation undergone by commercial TWCs and of their impact on total deactivation.

2. Experimental

2.1. Sample selection and manipulation

Since the chemical composition of TWCs and the level of deposition of contaminants may vary within the monolith, the axial and radial coordinates of the monolith whose specimens were studied here were carefully controlled. They were taken from the beginning (first 2 cm) of the upstream monolith (first cartridge) of Ford Focus 1.6 (1999 model) catalytic converters with ca. 44,000 and 66,000 km and also from a fresh catalyst. The distance to the central axis of the monolith was less than 3 cm. This area was chosen because higher contaminant concentrations are found at the beginning of the first monolith, facilitating the detection of phases containing the various contaminants (the radial gradient of contaminants is a less intense phenomenon) [10,11]. It was checked that the monoliths had been supplied by the same catalyst manufacturer, and that the specifications of the catalysts were similar in all the catalytic cartridges supplied. Moreover, the composition determined by TXRF regarding Al, Ce and Zr (mass ratio relative to Si) were similar in all catalysts (within the experimental error of the technique).

Small pieces of the ceramic wall with the adhered washcoat were obtained by gently breaking the monolith structure. An optimal physical shape (pieces of monolith wall or powder obtained by the grinding of such pieces) must be selected, depending on the characterisation technique to be used. The selection was made in order to facilitate the detection analyses, and emphasizing the chemical features brought about by the contamination of the aged TWC in question. Thus, the physical shape of the samples investigated will clearly be stated when describing the characterisation technique used. The catalyst with 0 km will be referred to as fresh and those with 44,000 and 66,000 km as u-44 and u-66, respectively.

2.2. Characterisation techniques

Nitrogen adsorption isotherms were recorded at the temperature of liquid nitrogen (77 K) using a Micromeritics ASAP 2000 apparatus. Prior to the determination of an adsorption isotherm, the sample was outgassed at 413 K for 12 h. N_2 adsorption isotherms were measured on finely ground samples.

TXRF analysis was performed on a Seifert EXTRA-II spectrometer (Rich Seifert & Co., Ahrensburg, Germany) equipped with two X-ray fine focus lines, Mo and W anodes, and a Si(Li) detector with an active area of 80 mm^2 and a resolution of 157 eV at 5.9 keV (Mn Kα). To carry out the TXRF analyses an X-ray tungsten source was used for P determination. Radiation was filtered with a Cu film of 10 μm thickness in order to optimise the energy range (0–10 keV) used in the analyses. The molybdenum X-ray source was used for the analysis of the rest of elements previously filtered with a Mo film of 50 μm. The exciting conditions used were a potential difference of 50 kV and a variable intensity, between 5 and 25 mA, to yield a count rate of about 5000 cps in the spectra acquired with the tungsten source and a potential difference of 50 kV and a variable intensity, between 5 and 30 mA, to yield a count rate of about 5000 cps in the spectra acquired with the molybdenum source. Ten milligram of a sample was ground to a powder of particle size less than 30 μm in an agate mortar. The powder was then further ground for 20 min in a vibrating micro-pulveriser having a ball and a base of agate; 1 ml of high-purity water was added to the powder. Next, the mixture was poured into a test-tube in which up to 2 ml of high-purity water was added. The sample was homogenized for 10 min by ultrasonic treatment in order to disperse the possible agglomeration of particles. Two microlitres of the suspension was placed on a flat carrier of plastic where the water was evaporated off under a vacuum. Further, details of the analysis are given elsewhere [10,11].

Powder X-ray diffraction patterns were recorded by scanning between 10° and 80° in the scan mode (0.02°, 2 s) using a Seiffert 3000 XRD diffractometer equipped with a PW goniometer with Bragg-Brentano $\theta/2\theta$ geometry, an automatic slit, and a bent graphite monochromator. Around 1 g of the small pieces of sample was finely ground before the pattern was recorded.

TPR studies were performed in an experimental device coupled to a Baltzer Prisma™ quadrupole mass spectrometer (QMS 200). Hundred milligrams of particles sieved between 0.60 and 0.80 mm, obtained by gently grinding the monolith walls, was loaded into a U-shaped reactor. Downstream from the catalytic bed, the lines were at temperatures higher than 313 K. Before the TPR experiment, the sample was calcined by heating at 773 K for 1 h (heating rate 10 K min^{-1}) under a 3% O_2/Ar flow (60 ml min^{-1}) and kept at 773 K for 1 h. Then, the sample was cooled down to room temperature under this mixture and switched to argon. After 1 h of treatment under flowing argon, the sample was cooled to 191 K also in a flow of argon. Finally, the gas flow was switched to a 2% H_2/Ar mixture, and a TPR–MS experiment was run in two steps: from 191 to 298 K, and then from 298 to 1173 K. The gas

flow rate was 50 ml min^{-1} and the heating rate 10 K min^{-1} (298–1173 K). In the 191–298 K range, the heating of the samples occurred freely.

2.3. Microactivity tests

Catalytic activity data were obtained using a conventional fixed-bed plug flow reactor at atmospheric pressure. A gas mixture was made up so that it would resemble the exhaust gas composition. In an attempt to mimic the oscillation (frequency around 1 Hz) of the exhaust gas composition due to the closed-loop control of the A/F ratio, the concentration of (CO, H_2 and O_2) was cycled at 1 Hz, oscillating at two different concentration values. The concentrations were CO_2 (10%, v/v), H_2O (10%, v/v), NO (900 ppm), C_3H_6 (900 ppm), CO, H_2, O_2 and Ar (balance) cycled between CO (0.4–1.6%, v/v), H_2 (0.13–0.53%, v/v) and (0.77–1.37%, v/v). These values define a central value for A/F = 14.63 and $\Delta\lambda = 0.03$ ($\lambda = (A/F)_{actual}/(A/F)_{stoichimetric}$) according to the equation described in Ref. [13]. Mass flow controllers were used to feed the gases and an HPLC pump was employed to feed the water. Electronically controlled fast valves, following the same strategies as those described by González-Velasco et al. [14–16], were used to achieve rapid selection between two different feed-streams.

Gases were preheated and water was pre-evaporated by cylindrical ovens set at 473 and 573 K, respectively, and placed upstream from the catalytic bed. The catalyst bed consisted of 1 ml of particles between 0.6 and 0.8 mm resulting from gently crushing the monolith and later mixed and diluted in 2 ml of SiC (particle size 0.5 mm). No separation of particles of different sizes was detected. Catalytic activity was measured at 10^5 h^{-1} in the light-off mode, raising the temperature from 373 to 973 K at 5 K min^{-1}. Different detectors connected on-line to the exit of the reactor were used. NO was detected using a chemiluminescence detector (HORIBA mod. CLA-510SS); CO and CO_2 were detected by dispersive infrared detectors (mod. HORIBA VIA-510), O_2 by a paramagnetic detector (mod. HORIBA MPA-510) and C_3H_6, H_2 and H_2O by a quadrupole mass spectrometer (mod. BALTZER Prisma QMS 200 controlled by BALTZER Quadstar™ 422 software).

3. Results

Fig. 1 shows the relative concentrations of some the most important contaminants deposited on the catalyst (phosphorous, zinc and lead). They were considered contaminants from the point of view of the composition of the TWCs because these atoms were present in the used samples and were absent or present in a much smaller concentration in the fresh sample. The additives of lubricating oil, burned in the combustion chamber of the engine, results in compounds that reach the exhaust pipe and deposit P and Zn in the

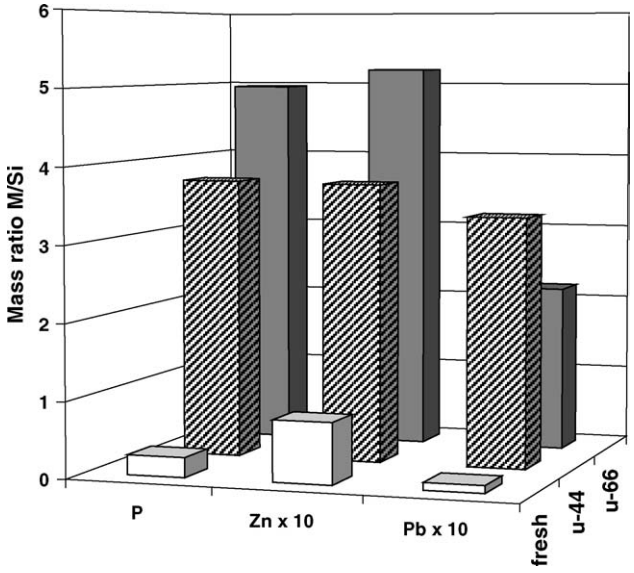

Fig. 1. Mass atomic ratio of elements M = (P, Zn and Pb) referred to Si as determined by TXRF.

catalyst. Silicon is a major element of cordierite, the ceramic material of which the monolith is constructed. Since Si is not a component of the washcoat, it is a suitable element for obtaining semi-quantitative information. It may be assumed that the Si concentration does not vary with mileage, since cordierite is not affected by aging and was therefore selected as a reference component. The level of contamination by Zn and Pb was one order of magnitude smaller than that afforded by P, so for the sake of clarity their mass ratios were multiplied by 10. Calcium is other very concentrated contaminant found in real used catalysts. Other techniques more appropriate than TXRF (Ca is major component of cordierite) have shown that Ca is a very common contaminant that is concentrated in a crust formed between Ca and other contaminants over the outermost layer of the washcoat [10]. Other contaminants, such as Ni, Cr, Cd and Cu, arising from the metallic part of the engine as a consequence of the tough conditions the engine is subjected to during functioning, can be also detected by TXRF but at concentrations almost two orders of magnitude smaller. In principle, their impact on deactivation can be considered much smaller than those of other more concentrated contaminants. It must also be stressed that no losses of Pd and Rh by attrition were detected. Fig. 1 shows that P and Zn deposition increased with mileage (and it is expected that Ca as well), which is perfectly consistent with the source and mechanism of deposition [8,9].

In principle, Pb should come from gasoline additives, but it may also arise from metallic parts of the engine or even from gasoline reservoir tanks. Although its content has been reduced by legislation in most European countries, Pb may still be present as trace impurities (few hundreds of ppm). It has been detected by chemical analyses carried out by the authors in different commercial gasolines (in fact, the level of Pb accumulation found in the present samples was of the

same order as that expected, assuming that all the Pb contained in the gasoline is burnt during use of the car and ends up deposited in the monolith). The deposition of Pb does not increase during use. It seems that the Pb content remains close to a certain value that does not depend on mileage, but instead on the specific operational variables under which the TWC is working (the Pb content in exhaust gases, temperature, flow pattern, flow rate, etc.). Statistically, such variables are similar as long as the car has accumulated enough mileage. This effect can be explained considering that Pb can form volatile compounds under the conditions that TWCs are subjected to (i.e. high temperature, halogen scavengers, etc.) [17]. In fact, the effect of Pb on TWCs disappears if Pb is completely absent from fuel [17].

Fig. 2 compares the XRD patterns of the used samples with that of the fresh sample. For the sake of clarity, only the most representative region of the diffraction angle ($2\Theta = 20^\circ$–35°) is shown. The intensity of the pattern was normalized to the peak at 2Θ ca. 21.8°: one of the reflections

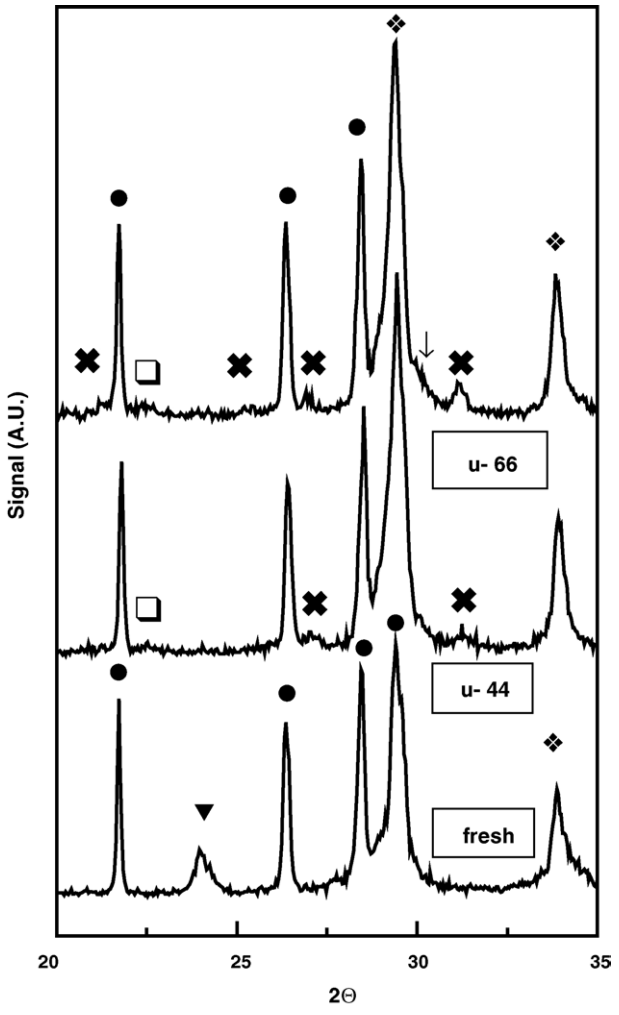

Fig. 2. XRD patterns of the samples. Symbols: (●) cordierite; (▼) tetragonal ZrO_2; (◆) Ce–Zr mixed oxide; (✖) $CePO_4$; (↓) and (❑) tentatively assigned to monoclinic and orthorhombic $Zn_2P_2O_7$.

of cordierite. This peak was chosen assuming that cordierite will not be significantly altered during ageing. The diffractogram of the fresh sample can be interpreted as arising from a mixture of cordierite (JCPDS file number 81-1387) (●) and tetragonal ZrO_2 (JCPDS file number 81-1329) (▼). The reference reported in this file corresponds to a stabilized zirconia [8,10,12]. The presence of a Ce–Zr mixed oxide (marked as ◆) cannot be discarded, as will be detailed below. The exact composition of the mixed oxide is beyond the scope of this study because it is proprietary, although a value close to 0.5 was estimated. The pattern of u-44 showed that reflections from the $Ce_{1-x}Zr_xO_2$ mixed oxide, now clearly distinguished from the cordierite reflections, became narrower and more intense. This effect can be explained in terms of a sintering of the particles of the $Ce_{1-x}Zr_xO_2$ mixed oxide and is in agreement with other results reported in the literature for both laboratory samples and commercial TWCs [8,18]. The ZrO_2 reflections disappeared, very probably at the expense of the formation of the Ce–Zr mixed oxide. Weak reflections from $CePO_4$ (✖) were also identified. On the other hand, the u-66 pattern was very similar to that of u-44, although two key differences were detected. First, the $CePO_4$ reflections were more intense. Since a larger concentration of P was found in the u-66 sample, greater mileage must bring about the formation of larger crystals of this Ce phosphate. Moreover, although its presence was incipient in u-44, a shoulder (↓) was evident at the right side of the most intense peak of the u-66 XRD pattern (at ca. $2\Theta = 30.2^\circ$). The position of this shoulder matched the most intense reflections of monoclinic $Zn_2P_2O_7$ (JCPDS file number 73-1648). $Zn_2P_2O_7$ has been reported to be present in other vehicle-aged TWCs studied by other groups [8,19]. The weak and broad peak at $2\theta = 22.46^\circ$ (marked as ❑ in Fig. 3) could correspond to the most intense reflection of orthorhombic $Zn_2P_2O_7$ (JCPDS file number 49-1240). No definitive assignment of those Zn pyrophosphate samples can be accomplished owing to the failure to detect other weaker reflections from these phases.

The used samples had a lower specific surface area than the fresh one (fresh = 17.8 $m^2\ g^{-1}$, u-44 = 7.5 $m^2\ g^{-1}$ and u-66 = 3.5 $m^2\ g^{-1}$). It must be taken into account that the samples contained cordierite and washcoat (alumina, Ce–Zr mixed oxides, noble metals and additives), and hence the volume of nitrogen adsorbed per gram of sample was smaller than the values expected for the washcoat alone. Ageing results in a decrease in the specific area and several phenomena can be invoked to explain this loss. Thermal sintering of the washcoat components is expected to occur in the aged TWCs due to the extreme conditions the catalysts are subjected to: water vapour at high temperatures. The sintering of Ce–Zr mixed oxide was evident in the XRD of our used samples. Sintering of Al_2O_3 and of noble metal was not detected by XRD (due to the lower intensity of their reflections), but cannot be discarded. The interparticle mesopores become larger when sintering develops larger agglomerates of oxide particles. This is consistent with the

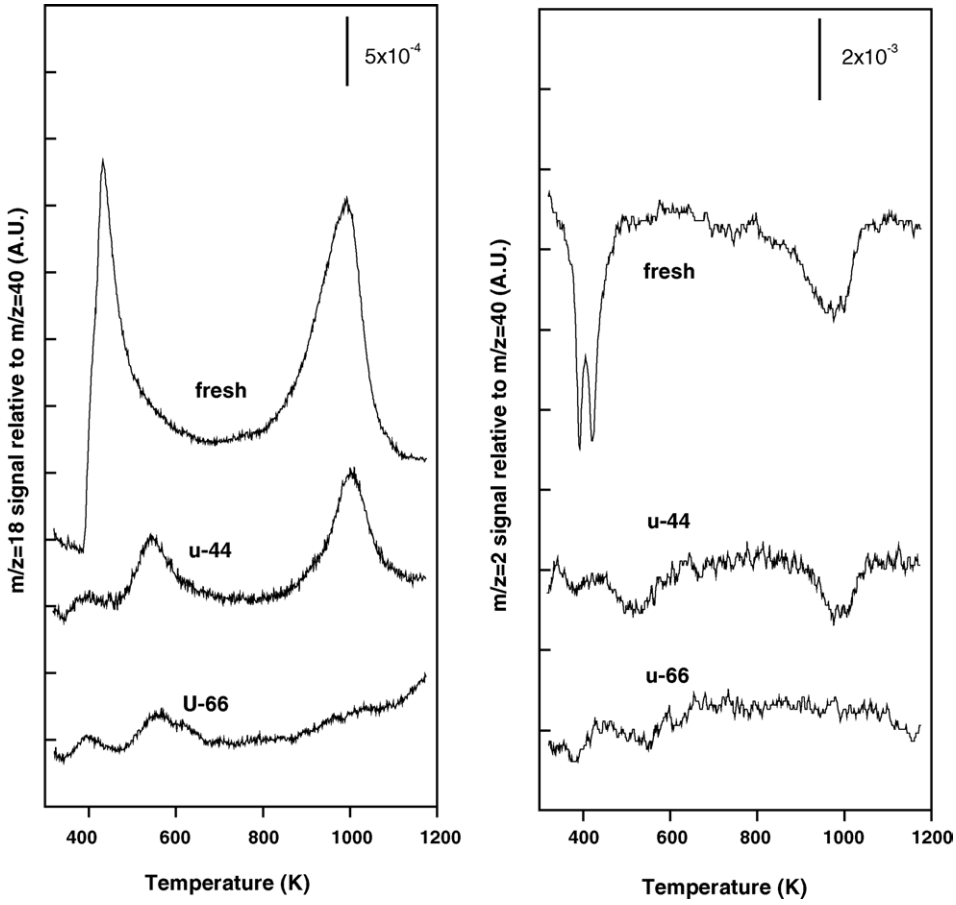

Fig. 3. TPR–MS profiles of the samples after oxidising pre-treatments at 773 K.

effects reported in laboratory scale studies, which have demonstrated that, at high temperatures, water vapour accelerates the rate of sintering [18,20]. Another explanation for the loss of specific area would be the presence of different phosphates. It has been reported that $MgZn_2(PO_4)_2$, $CaZn_2(PO_4)_2$, $Ca_3(PO_4)_2$, $Zn_3(PO_4)_2$ and $Zn_2P_2O_7$ species develop as an impervious amorphous layer of glaze on the TWC surface that fills and plugs the pores (particularly the smaller pores) [8,19,21]. Only $Zn_2P_2O_7$ was apparently detected by XRD in our TWCs, although the presence of other Ca and Mg phosphates cannot be ruled out. P may also be deposited in alumina pores, where it forms $AlPO_4$, which blocks the Al_2O_3 surface pores. Although $AlPO_4$ was not observed in the XRD study of our used catalysts, this effect cannot be discarded either. The above reasons, or a combination of them, can be invoked to explain the loss of surface area.

Fig. 3 shows TPR response curves obtained over the fresh and used TWC samples previously calcined at 773 K. Fig. 3 shows the ratio between the H_2O ($m/z = 18$) signal relative to Ar ($m/z = 40$) signal as a function of reduction temperature. H_2 consumption was also monitored ($m/z = 2$ signal), although its signal-to-noise ratio was considerable higher than that of H_2O due to the background level of $m/z = 2$ trace in the MS vacuum chamber. Fig. 3 clearly shows that H_2 consumption and H_2O evolution basically occurred simultaneously. This indicates that the re-adsorption of H_2O can be discarded as a key factor in defining the H_2O trace. Therefore, for the sake of simplicity and clarity, the discussion of the semi-quantitative aspects of TPR will be based on the H_2O trace. No H_2 consumption was detected when the H_2/Ar flow was switched to the reactor at 191 K, the latter immersed in an acetone refrigerant bath, or during heating from 191 to 300 K. This means that no reduction process occurs in this temperatures range. The assignments of the different reduction features shown in Fig. 3 could be accomplished based on the open literature, and in particular on research works concerning the reduction with hydrogen over pre-oxidised PGM metals (Pt, Pd and Rh) supported on alumina and on $Ce_{1-x}Zr_xO_2$ mixed-metal oxides (or on CeO_2). H_2O evolution measured in the TPR experiments arose from the concomitant reduction of the noble metal oxides (formed by the $5\%O_2$/He gas treatment), and of the Ce(IV) component of the Ce–Zr–O mixed oxide (or of the CeO_2) to Ce(III). However, it has been reported [22–28] that the method of catalyst preparation, the nature of the precursor used, the calcination temperature and other parameters critically affect the reduction of metal oxides present in a TWC. Therefore, definitive assignment of the reduction peaks observed in the present TWC samples is beyond the scope of this work and

should be taken with caution given the proprietary information concerning the exact chemical composition and initial state of the TWCs in question.

Nevertheless, it is important to note here that the amount of water evolved in the TPR experiments (and H_2 consumption) shown in Fig. 3 for the u-44 used TWC samples was considerably smaller than that obtained for the fresh sample, and in the case of u-66 sample it was even smaller. The low noble metal loading present in the TWC samples studied in this work, compared to the Ce oxide loading, renders the contribution of H_2O from the reduction step of the noble metal oxides quite small (the noble metal content was more than one order of magnitude smaller than the Ce content). In addition, the TXRF analysis of the fresh and used TWCs studied here revealed that the Ce content was similar in all TWCs. Therefore, the quantitative differences in the water signal observed in the TPR experiments shown in Fig. 3 cannot be explained by any loss of precious metal or cerium content and another explanation must be sought.

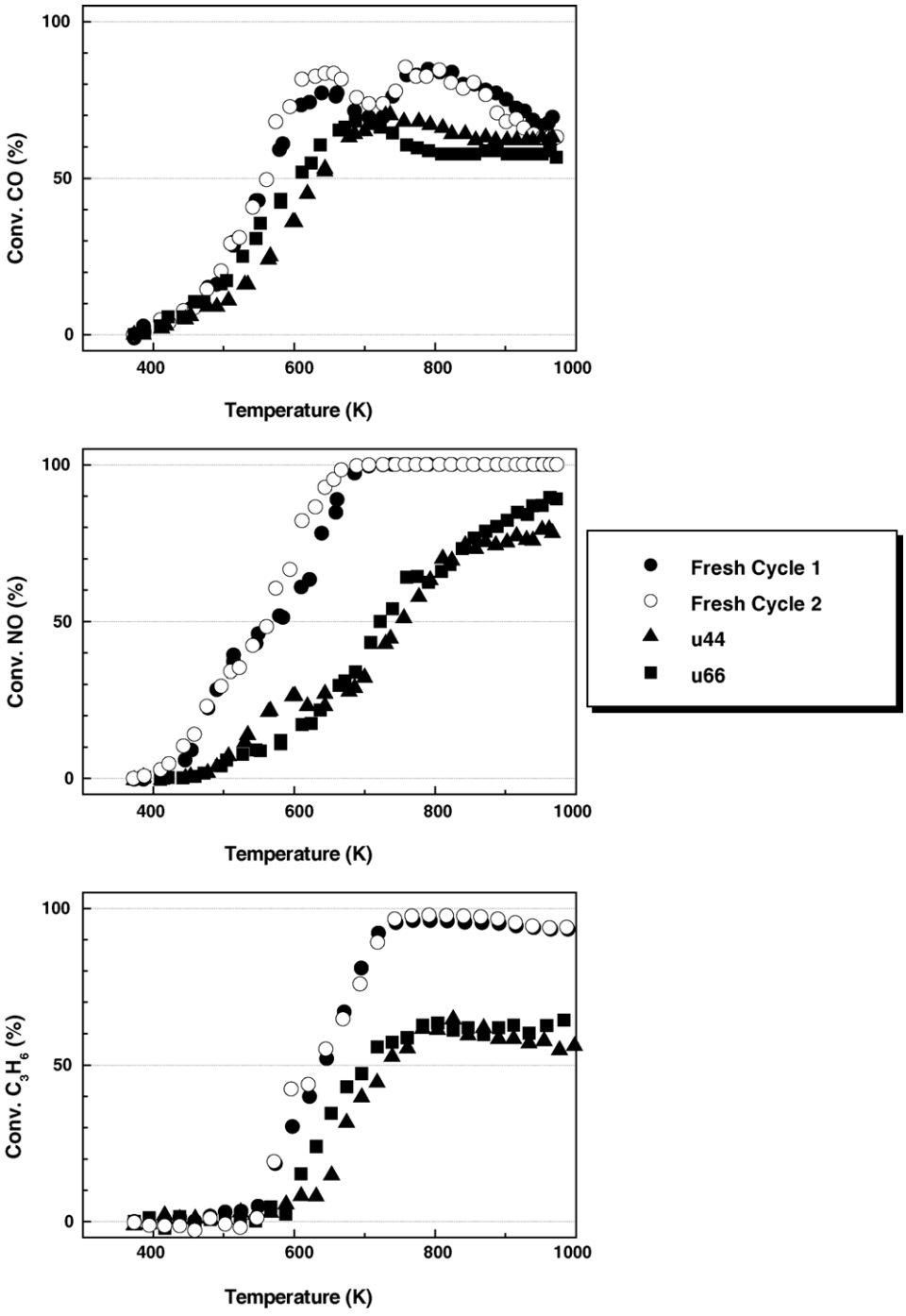

Fig. 4. Light-off curves for NO reduction and C_3H_6 and CO oxidation of the fresh and used samples.

The decrease in the amount of H_2O evolution observed in the TPR curve of the used samples with respect to the fresh one suggests that a smaller amount of Ce(IV) had been reduced. Two reasons can be envisaged to explain this effect. The first is that a smaller amount of Ce(IV) was readily available for reduction in the used sample as compared to the fresh one. It should be noted that although the presence of other amorphous Ce phosphates (not XRD visible) cannot be ruled out, the small amount of $CePO_4$ detected by XRD is insufficient to account for the lower amount of H_2O observed in the TPR spectra of the used TWC samples. However, a second, and more plausible reason is that the kinetics of the reduction with hydrogen of Ce(IV) to Ce(III) might have been altered in the used TWC when compared with that of the fresh TWC sample, characterised by a faster reduction rate of Ce(IV) to Ce(III). Although only a small amount of Ce appeared as Ce(III) in the $CePO_4$ phase, Ce(III) phosphate partly covered the Ce–Zr–O mixed oxide and the CeO_2 particles. The Ce(IV)/Ce(III) redox process is still possible at the subsurface region of Ce–Zr–O mixed oxide and CeO_2 but the presence of a Ce phosphate layer may reduce the rates of the reduction and reoxidation processes [29].

Regarding the total oxidation of CO and C_3H_6 and the reduction of NO, the catalytic activity of the fresh catalyst and of the u-44 and u-66 samples is shown in Fig. 4. A second cycle carried out on the fresh sample after cooling down to 373 K under an Ar flow (100 ml min^{-1}) replicated the CO, NO and C_3H_6 light-off curves, indicating the good reproducibility of the experiments. The profiles of the reaction observed in the figures can be explained by taking into consideration the conclusions of other groups that have made in-depth studies of the different mechanisms involved in the elimination of CO, NO and HC using similar feedstreams [14,16]. However, more relevant is the extent of deactivation in the used catalysts. The impact of use under traffic conditions on deactivation was evident in the used u-44 catalyst. From Fig. 4, it is clear that deactivation was remarkable for the reduction of NO, since the curve of the u-44 sample was shifted towards higher temperature with respect to that of the fresh sample and, moreover, conversion at 973 K was significantly smaller than that of the fresh sample. For the same reasons explained above, deactivation was also very intense for C_3H_6 oxidation. However, it was not so significant for CO oxidation. Regarding the degree of deactivation in the u-66 sample, the behaviour was fairly similar to that of the u-44 sample: deterioration was significant for NO reduction and for C_3H_6 oxidation, and not so remarkable for CO oxidation. It is worth noting that the light-off curves of the u-66 and u-44 samples were very similar, which means that the degree of deactivation in both samples was in fact similar. Therefore, although deactivation may increase with mileage, it seems that the rate of deactivation is more intense at low-mileage and slows down at higher mileage.

4. Discussion

Detection of the probable causes of deactivation is only one step in understanding the deactivation mechanisms of TWCs. An assessment of whether an effect is really deactivating the catalysts and an estimation of its impact are the essential tasks. The complex formulation of real catalysts, together with the diverse accumulated effects brought about in used TWCs under traffic conditions exacerbates the problem. Thus, critical evaluation of the effect of mileage on the deactivation of catalytic properties and on the effects detected in the used TWCs may provide some clues.

The characterisation of the vehicle-aged TWCs studied here revealed that the surface area of the used catalysts was smaller than that of the fresh catalyst and that the specific area of u-66 was even lower than that of u-44. On the other hand, P, Zn and Pb were deposited on the used TWCs; the P and Zn concentrations increased with mileage, whereas Pb did not but, instead, decreased. P was by far the most concentrated contaminant deposited on the catalyst. The diffraction peaks for $CePO_4$ (and very likely ZnP_2O_7) were detected by XRD and their intensities in u-66 with respect to those from other diffraction peaks were higher than in u-44. Previous effects must therefore affect the catalytic properties of the used TWCs, and indeed the results on catalytic activity showed that the used catalysts were deactivated and that in fact the deactivation of performance in CO oxidation was not as strong as in the case of NO reduction and propylene oxidation reactions. In addition, it seemed that the rate at which TWCs deactivate is stronger at low-mileage than at high-mileage.

However, the more intense loss of specific area did not result in a stronger deactivation of the catalytic properties at higher mileage. It may therefore be concluded that although the depletion of specific area due to either thermal effects or contaminant deposition may participate in deactivation, its impact on the worsening of catalytic properties cannot be the most important issue. Our results are in agreement with those of Beck et al., who have shown that thermal deactivation has a limited influence on the deactivation of NO and CO conversions, whereas their influence in the deactivation of HC oxidation is much smaller [9]. Our findings are also consistent with those of González-Velasco et al., who showed that Pd–Rh-based TWCs display the lowest degree of deactivation due to thermal aging [30].

The loss of specific area by thermal sintering is only one of the different thermal effects that may appear in aging under high temperature (other aspects can be found in [31,32]), but there is accumulating evidence to suspect that thermal effects only play a minor role in the deactivation of TWCs. Especially, in last generation of TWCs that contain Ce–Zr with an extraordinary oxygen storage capacity (OSC), yet maintained even sintering at high temperatures [6,26,27,30]. Therefore, we assign a restricted impact of

specific area depletion on the deactivation of TWCs, at least as regards thermal effects.

P and Zn deposition can also contribute to the loss of specific area. Beck et al. have shown that the effect of P and Zn deposition on the deactivation of catalytic properties is crucial in HC conversion and less important in CO and NO elimination [9]. Those authors claim that the glassy material developed between P, Zn (and Ca) and the washcoat components blocks access to the active sites. Phases formed between contaminants and washcoat components or between the contaminants themselves, such as $AlPO_4$ phases, $MgZn_2(PO_4)_2$, $CaZn_2(PO_4)_2$, $Ca_3(PO_4)_2$ and $Zn_3(PO_4)_2$, which have been detected by other groups in real used samples [8,19,33], have been claimed to be responsible for this glassy crust. In the samples studied here, incipient ZnP_2O_7 seemed to be formed. However, the formation of this layer can also be ruled out as an important source of deactivation, at least at higher mileage (it is possible that the glaze-like material was not as impervious as proposed). Otherwise, it would not be possible to understand the contradiction between the higher P and Zn concentration (and very likely that of Ca) and the similar catalytic properties of the u-44 and u-66 catalysts.

$CePO_4$ was observed by XRD in the used catalysts. The relevance of the detection of this phase results from the stability against oxidation of this Ce^{3+} phase [34,35]. The performance of TWCs under rich and poor O_2 oscillations in the composition of the exhaust gas is based on the buffering effect supplied by the rapid Ce^{4+}/Ce^{3+} redox couple. If Ce^{3+} is locked as $CePO_4$, the OSC of used catalysts will undergo substantial damage. In fact, only a small fraction of the Ce^{4+} of the u-44 and u-66 catalysts was susceptible to be reduced, as seen from a comparison of their TPR patterns with that of the fresh catalyst. The lower amount of Ce^{4+} that can be reduced has been related to the presence of very stable Ce^{3+} in $CePO_4$ [10,12,29]. The noteworthy effect that only a small amount of $CePO_4$ has on the reducibility of Ce suggests that a layer (or islands) of $CePO_4$ is developed on the Ce–Zr mixed oxide. The layer of Ce^{3+} necessarily arrests the progress of the reduction toward the interior (bulk) of the particle [10,12,29].

Although $CePO_4$ can be invoked to explain the smaller amount of H_2O evolved in TPR, it must be taken into account that thermal aging may also be involved in the alteration of the TPR pattern in the same direction as $CePO_4$ [22,26,27,36,38]. The results concerning the effect of thermal aging on the amount of Ce^{4+} that can be reduced in TPR experiments are controversial: no effect or a depletion of the amount of Ce^{4+} that can be reduced have been both reported in thermally aged Ce–Zr mixed oxide [22,26,27,36–38].

In any case, if it is accepted that the TPR pattern provides information about the extent of OSC damage, it can be argued that the u-44 sample would be less active than the fresh sample because the OSC would be damaged by inhibition of the Ce^{4+}/Ce^{3+} redox couple through the formation of $CePO_4$. A higher amount of $CePO_4$ was detected in the u-66 sample and its TPR indicated that a much smaller amount of Ce had been reduced. However, its catalytic activity was not further deteriorated than that of u-44. This suggests that although $CePO_4$ formation may participate in the deactivation of TWC catalysts, its contribution does not increase with longer times under vehicle aging. This observation minimizes the impact of $CePO_4$ as a source of deactivation, especially at high-mileage.

Despite the foregoing, deactivation due to the formation of $CePO_4$ cannot be fully ruled out because saturation of the inhibition by Ce phosphate may occur. Such saturation can be rationalised as follows: a small amount of $CePO_4$ forms a layer and a barrier for the oxygen exchange that is sufficient to damage and block the OSC at low-mileage. In fact, as explained above, only a small fraction of the $CePO_4$ seems to alter the TPR behaviour dramatically. Additional, $CePO_4$ formation due to longer times under P deposition may merely thicken the Ce phosphate layer, with no observable effect on the TPR and OSC properties.

As a final point, the chemical analyses revealed that the Pb deposition was fairly similar in the u-66 and in the u-44 samples. The deactivation of activity followed a similar trend: the catalytic activity of u-66 was quite similar to that of u-44 in all the reactions catalysed by the TWCs. In view of this coincidence Pb had the strongest impact on the deactivation of the TWC catalysts studied here. Pb has been reported to form an alloy with noble metal(s) and to poison the active sites involved in the network of reactions that occur in TWCs that lead to the elimination of NO, HC and CO [39]. Research at our laboratory is currently under way to clarify the role of Pb poisoning in model TWCs. Although Pb plays a major role in the deactivation of TWCs, the participation of $CePO_4$ and of ZnP_2O_7 cannot be completely discarded at low-mileages. In fact, the catalytic properties of the catalyst with the highest mileage, u-66, could primarily be defined by the impact of Pb poisoning, with minor contributions from $CePO_4$ formation and from P and Zn deposition (the depletion in specific area cannot be forgotten, although its impact is even lower). As a result, the u-66 sample was as active as the u-44 catalyst because the Pb concentration was also similar. Finally, it should be briefly mentioned that none of the effects caused by the working conditions resulted in any important deactivation of the CO oxidation reaction. The effects on NO reduction and on propylene oxidation were much more severe.

Although the choice of vehicle-aged TWCs at different mileages was made under the reasonable assumption that driving conditions are statistically similar in the low- and high-mileage used TWCs studied here, a bench-aging procedure would be needed to minimize the uncontrolled effects that may occur in real traffic-aging. However, what it is certain is that although the differences in the effects detected in the u-44 and u-66 may arise from variations in the driving conditions instead of from an increase in the

time-on-stream effect (higher mileage), one is still dealing with catalysts with the same composition affected by the same effects but with different intensities. Considering this, the conclusions are still valid, although the hypothesis of the slowing down of the deactivation rate should be verified on bench-engine dynamometers.

5. Conclusions

A study of the effect of mileage on the degradation of TWC catalysts under vehicle aging conditions has been carried out. Working under traffic conditions results in the deactivation of TWCs. The strongest deactivation occurred in C_3H_6 oxidation and NO reduction. Deactivation of the CO oxidation reaction was much less severe. The rate of deactivation was higher at lower mileage; the rate of degradation seemed to decrease as mileage increased. Among the effects induced by the working conditions (a decrease in specific area, the formation of $CePO_4$ and of $Zn_2P_2O_7$, a depletion of the amount of Ce^{4+} available for reduction, and P, Zn and Pb deposition) the only effect that did not increase with mileage was Pb deposition. Thus, it may be concluded that Pb poisoning exerts the defining impact on the deactivation of catalytic activity. The other effects may play a secondary role and complete the deactivation due to Pb poisoning.

Acknowledgements

The financial support from Comunidad de Madrid is gratefully acknowledged for funding the project (7M/0081/2002). FCG also thanks the Spanish Ministry of Science and Education for a fellowship. The authors also wish to express their gratitude to Mr. Ramón Tomé for his invaluable help in the extraction of the monoliths.

References

[1] P. Greening, Top. Catal. 16 (2001) 5.
[2] R.M. Heck, R.J. Farrauto, S. Gulati, Catalytic Air Pollution Control. Commercial Technology, John Wiley & Sons Inc., New York, 2002
[3] M. Shelef, R.W. McCabe, Catal. Today 62 (2000) 35.
[4] A. Martínez-Arias, M. Fernández-García, A.B. Hungría, A. Iglesias-Juez, K. Duncan, R. Smith, J.A. Anderson, J.C. Conesa, J. Soria, J. Catal. 204 (2001) 238.
[5] S. Bernal, J.J. Calvino, M.A. Cauqui, J.M. Gatica, C.L. Cartes, J.A.P. Omil, J.M. Pintado, Catal. Today 77 (2003) 385.
[6] R. DiMonte, P. Fornasiero, J. Kăspar, M. Graziani, J.M. Gatica, S. Bernal, A. Gómez-Herrero, Chem. Commun. 21 (2000) 2167.
[7] R. Di Monte, P. Fornasiero, J. Kašpar, P. Rumori, G. Gubitosa, M. Graziani, Appl. Catal. B: Environ. 24 (2000) 157.
[8] M.J. Rokosz, A.E. Chen, C.K. Lowe-Ma, A.V. Kucherov, D. Benson, M.C.P. Peck, R.W. McCabe, Appl. Catal. B: Environ. 33 (2001) 205.
[9] D.D. Beck, J.W. Sommers, C.L. DiMaggio, Appl. Catal. B: Environ. 11 (1997) 257.
[10] C. Larese, F. Cabello Galisteo, M. López Granados, R. Mariscal, J.L.G. Fierro, M. Furió, R. Fernández-Ruiz, Appl. Catal. B: Environ. 40 (2003) 305.
[11] R. Fernández-Ruiz, M. Furió, F. Cabello Galisteo, C. Larese, M. López Granados, R. Mariscal, J.L.G. Fierro, Anal. Chem. 74 (2002) 5463.
[12] C. Larese, F. Cabello Galisteo, M. López Granados, R. Mariscal, J.L.G. Fierro, P.S. Lambrou, A.M. Efstathiou, Appl. Catal. B: Environ. 48 (2004) 113.
[13] E.S.J. Lox, B.H. Engler, in: G. Ertl, H. Knözinger, J. Weitkamp (Eds.), Environmental Catalysis-Mobile Sources, Wiley-VCH, New York, 1999, p. 1.
[14] J.R. González-Velasco, J.A. Botas, J.A. González-Marcos, M.A. Gutiérrez-Ortiz, Appl. Catal. B: Environ. 12 (1997) 61.
[15] J.R. González-Velasco, M.A. Gutiérrez-Ortiz, J.L. Marc, J.A. Botas, M.P. González-Marcos, G. Blanchard, Appl. Catal. B: Environ. 22 (1999) 167.
[16] J.A. Botas, M.A. Gutiérrez-Ortiz, M.P. González-Marcos, J.A. González-Marcos, J.R. González-Velasco, Appl. Catal. B: Environ. 32 (2001) 243.
[17] J.C. Guibet, Fuels and Engines, Technology, Energy, Environment, Editions Technip, Paris, 1999.
[18] M. Colon, F. Pijolat, H. Valdivieso, J. Vidal, E. Kăspar, M. Finocchio, C. Daturi, J.C. Binet, R.T. Lavalley, S. Baker, Bernal, J. Chem. Soc., Faraday Trans. 94 (1998) 3717.
[19] D.R. Liu, J.S. Park, Appl. Catal. B: Environ. 2 (1993) 49.
[20] C. Bozo, F. Gaillard, N. Guilhaume, Appl. Catal. A: Gen. 220 (2001) 69.
[21] W.B. Williamson, J. Perry, R.L. Goss, H.S. Gandhi, R.E. Beason, SAE Technical Paper 841406 (1984).
[22] P. Fornasiero, J. Kašpar, V. Sergo, M. Graziani, J. Catal. 182 (1999) 56.
[23] P. Fornasiero, J. Kašpar, M. Graziani, J. Catal. 167 (1997) 576.
[24] P. Fornasiero, G. Balducci, R. Di Monte, J. Kăspar, V. Sergo, G. Gubitosa, A. Ferrero, M. Graziani, J. Catal. 164 (1996) 173.
[25] C. Li, Y. Sakata, T. Arai, K. Domen, K. Maruya, T. Onishi, J. Chem. Soc., Faraday Trans. 85 (1989) 1451.
[26] G.W. Graham, H.W. Jen, R.W. McCabe, A.M. Straccia, L.P. Haack, Catal. Lett. 67 (2000) 99.
[27] H.W. Jen, G.W. Graham, W. Chun, R.W. McCabe, J.P. Cuif, S.E. Deutsch, O. Touret, Catal. Today 50 (1999) 309.
[28] S. Bernal, J.J. Calvino, G.A. Cifredo, J.M. Gatica, O. Prez, A. Laachir, V. Perrichon, Stud. Surf. Sci. Catal. 96 (1995) 419.
[29] C. Larese, F. Cabello Galisteo, M. López Granados, R. Mariscal, J.L.G. Fierro, P.S. Lambrou, A.M. Efstathiou, J. Catal. 226 (2004) 443.
[30] J.R. González-Velasco, J.A. Botas, R. Ferret, M.P. González-Marcos, J.L. Marc, M.A. Gutiérrez-Ortiz, Catal. Today 59 (2000) 395.
[31] L.A. Carol, N.E. Newman, G.S. Mann, SAE Technical Paper 892040 (1989).
[32] F. Maire, M. Capelle, G. Meunier, J.F. Beziau, D. Bazin, H. Dexpert, F. Garin, J.L. Schmitt, G. Maire, Stud. Surf. Sci. Catal. 96 (1995) 749.
[33] B. Angelé, K. Kirchner, Chem. Eng. Sci. 35 (1980) 2089.
[34] M. Tsuhako, S. Ikeuchi, T. Matsuo, I. Mutooka, M. Kobayashi, Bull. Chem. Soc. Jpn. 52 (1979) 1034.
[35] M. Tsuhako, S. Ikeuchi, T. Matsuo, I. Motooka, M. Kobayashi, Chem. Lett. 2 (1977) 195.
[36] M. Daturi, E. Finocchio, C. Binet, J.C. Lavalley, F. Fally, V. Perrichon, H. Vidal, N. Hickey, J. Kăspar, J. Phys. Chem. B 104 (2000) 9186.
[37] H. Vidal, S. Bernal, J. Kăspar, M. Pijolat, V. Perrichon, G. Blanco, J.M. Pintado, R.T. Baker, G. Colon, F. Fally, Catal. Today 54 (1999) 93.
[38] J. Kašpar, R. Di Monte, P. Fornasiero, M. Graziani, H. Bradshaw, C. Norman, Top. Catal. 16–17 (2001) 83.
[39] J. Goetz, M.A. Volpe, A.M. Sica, C.E. Gigola, R. Touroude, J. Catal. 167 (1997) 314.